Traceability of high focal length cameras with diffractive optical elements

2016 J. Phys.: Conf. Ser. 772 012005

(http://iopscience.iop.org/1742-6596/772/1/012005)

Traceability of high focal length cameras with diffractive optical elements

L Lages Martins[1], A Silva Ribeiro[1] and J Alves e Sousa[2]

[1]LNEC - National Laboratory for Civil Engineering, Lisbon, Portugal
[2]LREC - Regional Laboratory for Civil Engineering, Funchal, Madeira, Portugal

Corresponding author's e-mail address: lfmartins@lnec.pt

Abstract. This paper describes the use of diffractive optical elements (DOEs) for metrological traceable geometrical testing of high focal length cameras applied in the observation of large-scale structures. DOEs and related mathematical models are briefly explained. Laboratorial activities and results are described for the case of a high focal length camera used for long-distance displacement measurement of a long-span (2278 m) suspension bridge.

1. Introduction

The use of digital images for dimensional and geometrical measurements is increasing both in Science and Industry due to the technological developments occurred over the past decades in digital cameras and computers, which are now more accessible, reliable and with higher performance [1]. A camera permits a high quantity of information in a single image, including the dimension and geometrical shape of the observed object within a reduced timeframe interval, without contact, using a robust, real time automatized procedure.

In order to achieve high accuracy measurements, cameras are subjected to geometrical testing in order to estimate their intrinsic parameters – focal length, principal point image coordinates and distortion coefficients – which are required to be used as input quantities in the measurement process, with a direct impact on the metrological quality of the measurand.

In areas such as Photogrammetry and Computer Vision, which usually deals with reduced or normal focal length cameras (lower than 100 mm), this task is accomplished by conventional methods [2-5] supported in reference patterns or points. However, in the case of high focal length cameras, these methods often proved to be numerically unstable, providing unrealistic estimates for the intrinsic parameters. To overcome this limitation, several alternative approaches [6-7] have recently been proposed, e.g., the use of diffractive optical elements or DOEs.

This paper presents an innovative approach based on the use of DOEs to establish an accurate metrological traceability for geometrical testing of high focal length cameras, considering that this method has simplified setup requirements, if compared with laboratorial testing using high accuracy goniometers, and is more accurate than the complex approach of field testing with reference points [6]. Following a brief description about the geometrical testing of cameras using DOEs, the paper presents its application in the characterization of a high focal length (600 mm) camera used for displacement measurement in a long-span (2278 m) suspension bridge: the 25th of April Bridge (P25A), in Lisbon (Portugal). Estimates and measurement uncertainties, obtained by a Monte Carlo Method [8] in a non-linear, multivariable and complex optimization process, are discussed and a sensitivity analysis is performed to identify the main contributions for the measurement uncertainty evaluation.

2. Camera geometrical testing by the DOE method

The DOE method is supported in a collimated laser beam which passes through a DOE, creating a known spatial pattern of diffraction dots in the camera's focal plane. The DOE, usually a diffraction grating, has a complex microstructure with two or several depth levels produced by photolithography, which leads to a high accuracy spatial period.

The knowledge of the laser wavelength, the DOE spatial period and the diffraction dots image coordinates is used to determine the camera's intrinsic parameters – focal length, principal point image coordinates and distortion coefficients – through a non-linear optimization process which aims at the minimization of the following function [7]

$$\min_m \left\| \begin{bmatrix} \hat{u} - u_0 \\ \hat{v} - v_0 \end{bmatrix} - f \begin{bmatrix} x \\ y \end{bmatrix} [1 + k_1 \cdot (x^2 + y^2) + \cdots] \right\|^2 \quad (1)$$

being the unknown variables described m given by the following vector,

$$m = [f, u_0, v_0, k_1, \omega, \psi, \kappa, \alpha, \beta] \quad (2)$$

where $(\hat{u}, \hat{v})$ and (x, y) are, respectively, the diffraction dots distorted and ideal image coordinates, f is the camera's focal length, (u_0, v_0) are the principal point image coordinates, k_1 is the first-order radial distortion coefficient, (ω, ψ, κ) are the camera's orientation Euler angles and (α, β) are the DOE orientation angles with respect to the collimated laser beam coordinate system.

This method has proven to be suitable for the geometrical characterization of reduced focal length cameras [7]. However, no information is available about its application to high focal length cameras, thus justifying this study. This type of cameras is quite relevant for long-distance observation of large-scale structures since they contribute to a high displacement measurement sensitivity.

3. Experimental setup

Based on the main features of the tested camera (see Table 1), an experimental setup was developed in a laboratorial optical bench for the implementation of the DOE method, as shown in Figure 1.

Table 1. Camera components

Component	Description
Image sensor	Visible and near-infrared CCD; 7.4 μm squared pixel; (1920 × 1080) pixels
Frame grabber	PCMCIA interface; Imperx Framelink Application
Telephoto lens	Sigma, 300 mm/2.8 APO EX DG
Optical converter	Sigma, APO 2× EX DG

In a first stage, the experimental testing was made only with the 300 mm lens and in a second stage with the converter assembled in order to evaluate the influence of this component. Due to a manual infinity focus adjustment ring on the lens, additional studies were also performed – image acquisition with different focus positions – to determine its impact on the intrinsic parameters repeatability.

The DOE selected for this study was a diffraction grating (Holoeye, model DE-R-241, 8 mm diameter and a thickness of 1.2 mm) capable of producing a 21 × 21 dots matrix pattern, with a total diffraction angle of 4.8º and a spatial period estimate equal to 152.4 μm. This grating is optimized for a laser wavelength of 635 nm, which results in the lowest intensity increase (about 0.3%) of the central (zero order) diffraction spot. Since the total diffraction angle produced by the diffraction grating was higher than the camera's field of view, not all of the diffraction orders were observed, as shown in Figures 2 and 3.

The main operational concerns were related to laser beam attenuation by the use of a neutral filter (to avoid saturation and sensor damage) and the optical alignment which has a direct impact on the

profile quality of the diffraction orders irradiance (absence of unwanted effects such as defocusing, reflections, diffraction fringes, non-collimated and non-Gaussian beam).

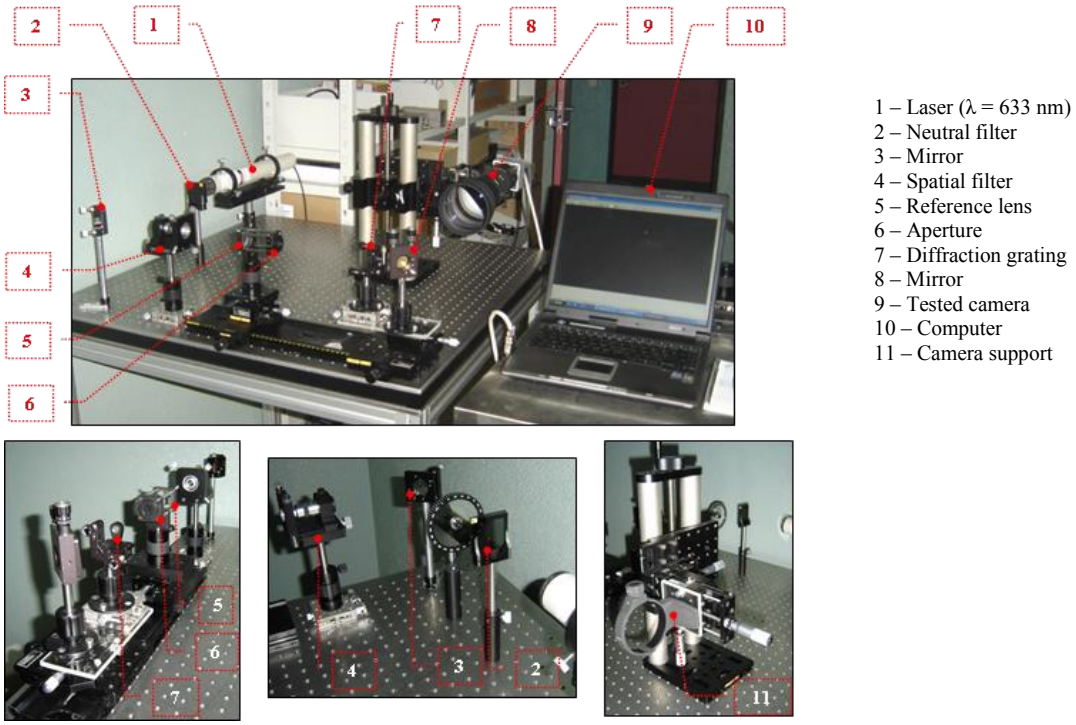

Figure 1. Experimental setup for the laboratorial implementation of the DOE method.

Figure 2. Observed diffraction pattern for the telephoto lens (without converter assembly).

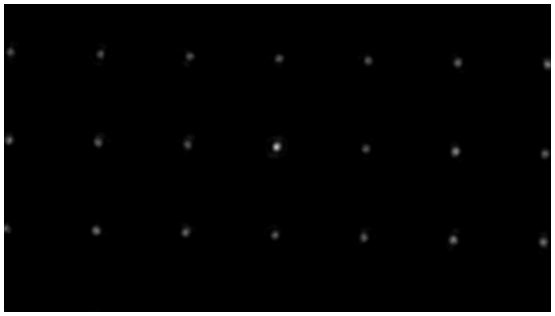

Figure 3. Observed diffraction pattern for the telephoto lens and converter assembly.

The obtained images were subjected to digital processing – thresholding for binary conversion, followed by opening morphological operation with a disk as the structuring element and Gaussian adjustment – aiming at the determination of the dots image coordinates. The obtained estimates were used as input quantities, as well as the laser wavelength and the diffraction grating spatial period estimates, in a non-linear optimization process.

This calculation task was supported in the Nelder-Mead simplex algorithm [9] dedicated to multivariable functions, such as equations (1) and (2), using a direct search method in which the calculation of numerical or analytical gradients are not required. Initial values for the unknown variables were defined based on nominal or approximated values, and were kept constant for both the two studied cases (300 mm or 600 mm focal length assemblies). A 10^{-6} pixel^2 stopping criterion was defined for the objective function given by equations (1) and (2).

4. Results and discussion

Tables 2 and 3 summarize the obtained results – average values and experimental standard deviations – for the camera's intrinsic parameters, noticing that a total of five images of the diffraction pattern were acquired for each infinity focus position. With respect to the lens distortion, only the first-order radial distortion coefficient was accounted in equations (1) and (2), since this type of optical aberration is known to be reduced for the case of high focal length lenses.

Table 2. Focal length and first-order radial distortion coefficient.

Intrinsic parameter	f / mm		k_1 / 10^{-6} m^{-2}	
∞ focus position	Lens	Lens & converter	Lens	Lens & converter
A	300.1±1.4	590.9±2.2	110±32	-102±51
B	300.9±0.5	604.8±4.9	69±9	76±32
C	301.7±0.2	597.0±2.1	80±11	9±17

Table 3. Principal point image coordinates.

Intrinsic parameter	u_0 / pixel		v_0 / pixel	
∞ focus position	Lens	Lens & converter	Lens	Lens & converter
A	532.6±2.4	566.2±2.1	996.5±2.9	954.2±3.7
B	536.3±0.8	533.8±1.7	1012.7±1.1	965.4±2.5
C	534.5±1.0	546.9±2.2	1012.5±1.3	963.3±4.4

The results obtained for the focal length parameter are closer to the expected nominal values, however, in the case where the converter is used, the deviation to the 600 mm nominal value and the corresponding experimental standard deviations are higher. This is justified by the reduced number of observed diffraction dots and by the mechanical assembly of the two optical components. The influence of the infinity focus position is also more noticed when the converter is mounted on the lens, namely, for position B.

Regarding the first-order radial distortion coefficient, estimates varied between -102×10^{-6} m^{-2} and 110×10^{-6} m^{-2} with experimental standard deviations ranging from 9×10^{-6} m^{-2} up to 51×10^{-6} m^{-2}. Although having a wide variation interval, the estimates magnitude is insufficient to affect the accuracy of the diffraction dot's image coordinates (lower than 0.01 pixel). This result confirms the reduced effect of radial distortion in high focal length lenses and allows the removal of this strongly non-linear component from the optimization processes (intrinsic parameterization and displacement measurement), thus increasing its numerical stability. Radial distortion differences between the two tested assemblies are mainly noticed in the extreme focus positions (A and C), with a reduced impact on the image coordinates accuracy.

Estimates for the principal point image coordinate in the x-direction are close to the expected 540 pixel nominal value, for both tested assemblies, and the magnitude of the corresponding experimental standard deviations is also similar for the studied infinity focus positions. A minimum dispersion value is always obtained for the intermediate focus position (B) for both principal point image coordinates (u_0, v_0).

Significant differences were found between the two tested assemblies in the estimates of the principal point image coordinate in the y-direction (v_0), noticing that the lens and converter assembly

presents results close to the 960 pixel nominal value. This can be justified by incorrect centering of the observed diffraction pattern in the y-direction of the camera without the converter, as seen in Figure 2, where the zero-order diffraction dot is not correctly centered in the middle of the image acquired.

Due to the non-linear nature of the optimization process, a Monte Carlo method [8] was applied for the determination of the measurement uncertainty of the estimated intrinsic parameters. This computational algorithm was developed in Matlab using validated functions and the Mersenne Twister pseudorandom number generator [10]. For each simulation, a total of 10^4 trials were performed in order to obtain convergent solutions. For this case, an iterative procedure was implemented and convergent solutions were obtained considering that the result of a Monte Carlo simulation updated the initial values of the following non-linear optimization.

The standard uncertainties related to the diffraction dot's image coordinates (ranging from ¼ up to ¾ of a pixel) and to the diffraction grating spatial period (0.15 µm) were propagated to the output quantities (the laser wavelength quantity was considered constant). The 95% expanded uncertainty of the focal length parameter was found between 0.75 mm and 1.9 mm. Regarding the principal point coordinates, the 95% expanded uncertainty ranged between 0.06 pixel and 0.21 pixel. Correlation effects were noticed between intrinsic parameters (correlation coefficients between -0.35 and -0.25).

The performed sensitivity analysis revealed the diffraction dot's image coordinates as the major contribution (close to 75%) for the output measurement uncertainty, reflecting the impact of input uncertainties components related to digital image processing and laser beam collimation quality.

The studied camera (with the 300 mm lens and converter assembly) was later applied in the measurement of the displacement of the main span central section of the P25A Bridge (Fig. 4 and 5).

Figure 4. P25A suspension bridge in Lisbon (Portugal).

Figure 5. Camera installed in the P25A suspension bridge main span central section.

In this approach, the camera was rigidly connected to the lower region of the stiffness beam and orientated towards the tower foundation, establishing an estimated observation distance of 510 m. A geometric referential composed by four active targets, with known world coordinates, was placed in a bridge tower foundation (Figure 4), visible for the camera range in the main span central section.

In this condition, changes of the camera's projection center world coordinates are considered representative of the bridge displacement and can be determined by non-linear optimization using as input quantities the targets image and world coordinates (obtained from digital image processing and previous laboratory dimensional testing, respectively) and the camera's intrinsic parameters (by previous laboratory testing, as described in this paper).

Maximum vertical and transverse displacements of 1.62 m and 0.29 m were measured with a 95% expanded uncertainty comprised between 4 mm and 7 mm, for the observed environmental conditions (Summer and Winter measurement campaigns). For this case, the performed sensitivity analysis revealed that the contribution of the intrinsic parameters (focal length and principal point image coordinates) ranged from 15% up to 24% of displacement measurement uncertainty.

5. Conclusions

This study enabled the conclusion that the DOE method is suitable for metrological traceable geometrical testing of high focal length cameras, at least, up to 600 mm, without any numerical instability in the optimization process, as it often occurs when conventional methods are applied. Radial distortion revealed to be negligible not affecting significantly the image coordinates accuracy. This in turn permitted the removal of this strongly non-linear component from the optimization, therefore, contributing for the achieved numerical stability of the parameterization and measurement processes.

The camera with the 600 mm focal length assembly was used in the structural observation of the P25A Bridge. Although the obtained estimates and measurement uncertainties of the camera's intrinsic parameters contributed for about 15% to 24% of the final displacement accuracy, other input quantities of the mathematical model such as the targets image coordinates (55% - 58%) and target world coordinates (18% - 30%) coordinates showed higher contributions to the output uncertainty.

The DOE method can now be used to identify the occurrence of any damage or drift effect in the camera, namely, in permanent observation scenarios, due to the long-term exposure of the camera to an aggressive dynamic environment.

Acknowledgments

The authors gratefully acknowledge José Rebordão, Manuel Abreu and Fernando Monteiro from the Laboratory of Optics, Lasers and Systems of the *Faculdade de Ciências da Universidade de Lisboa* which contributed for the experimental setup and discussion of intrinsic parameterization results.

This work was funded by the Portuguese Ministry of Education and Science National Funds through FCT-Foundation for Science and Technology, under PhD research grant ref. SFRH/BD/76367/2011 assigned to L Lages Martins.

The project I&D UID/MAT/04674/2013 of FCT-Foundation for Science and Technology, supported J Alves e Sousa's contribution, and is grateful acknowledge.

References

[1] Schwenke H, Neuschaefre-Rube U, Pfeifer T, Kunzmann H, 2002 *CIRP Annals – Manufacturing Technology*, **51**, 2, 685-699
[2] Abdel-Aziz Y, Karara H, 1971 *Proceedings of the Symposium on Close-Range Photogrammetry*, 1-18
[3] Heikkilä J, Silvén O, 1997 *Conference on Computer Vision and Pattern Recognition – Proceedings CVPR 1997*
[4] Tsai R, 1987 *IEEE Journal of Robotics and Automation*, **RA-3**, 4
[5] Zhang Z, 2000 *IEEE Transactions on Pattern Analysis and Machine Intelligence*, **22**, 11
[6] Hieronymus J, 2012 *International Archives of Photogrammetry, Remote Sensing and Spatial Information Sciences*, **XXXIX-B5**
[7] Bauer M, Grießbach D, Hermerchmidt A, Krüger S, Scheele M, Schischmanow A, 2008 *Optics Express*, **16**, 25
[8] *S1-GUM Evaluation of measurement data. Supplement 1 to the "Guide to the expression of Uncertainty in Measurement". Propagation of distributions using a Monte Carlo method"*, 1st edition, JCGM, 2008
[9] Lagarias J, Reeds J, Wright P, 1998 *SIAM Journal of Optimization*, **9**, 1, 112-147
[10] Matsumoto M, Nishimura T 1998 *AMC Transactions on Modeling and Computer Simulation*, **8**, 1, 3-30